Atom-light superposition oscillation and Ramsey-like atom-light interferometer

Cheng Qiu[1], Shuying Chen[1], L. Q. Chen[1,*], Bing Chen[1],

Jinxian Guo[1], Z. Y. Ou[1,2,†], and Weiping Zhang[1,‡]

[1] *Department of Physics, East China Normal University, Shanghai 200062, P. R. China*

[2] *Department of Physics, Indiana University-Purdue University Indianapolis, 402 North Blackford Street, Indianapolis, Indiana 46202, USA*

This is the author's manuscript of the article published in final edited form as:

Qiu, C., Chen, S., Chen, L. Q., Chen, B., Guo, J., Ou, Z. Y., & Zhang, W. (2016). Atom–light superposition oscillation and Ramsey-like atom–light interferometer. Optica, 3(7), 775-780. https://doi.org/10.1364/OPTICA.3.000775

Coherent wave splitting is crucial in interferometers. Normally, the waves after this splitting are of the same type. But recent progress in interaction between atom and light has led to the coherent conversion of photon to atomic excitation. This makes it possible to split an incoming light wave into a coherent superposition state of atom and light and paves the way for an interferometer made of different types of waves. Here we report on a Rabi-like coherent-superposition oscillation observed between atom and light and a coherent mixing of light wave with excited atomic spin wave in a Raman process. We construct a new kind of hybrid interferometer based on the atom-light coherent superposition state. Interference fringes are observed in both optical output intensity and atomic output in terms of the atomic spin wave strength when we scan either or both of the optical and atomic phases. Such a hybrid interferometer can be used to interrogate atomic states by optical detection and will find its applications in precision measurement and quantum control of atoms and light.

In quantum storage, complete conversion of quantum states between atoms and light is essential for the high fidelity transfer of quantum information. Quantum storage was first realized with the method of electromagnetically induced transparency [1–6]. More recently, Raman processes were used to achieve wide band quantum storage [7–9]. On the one hand, most researches concentrated on increasing the efficiency of quantum storage because a partial conversion is usually regarded as a loss for the quantum system and leads to a reduction in the fidelity of quantum information transfer. But the unconverted part still contains the original information. So, if available, it can be further converted [10] for better overall conversion efficiency. On the other hand, since quantum storage is coherent in the sense that the phase of the quantum states is preserved, the converted and the unconverted parts are coherent to each other. This property can be employed for quantum interference. Indeed, Campell et al [11] achieved coherent mixture of atomic wave and optical wave in a atom-photon polariton state with gradient echo memory scheme.

Rabi oscillation is a coherent population oscillation between two atomic levels when driven by a strong coherent radiation field coupled to the two levels [12]. It played an important role in atomic clocks by forming a Ramsey atomic interferometer [13]. Two-photon Rabi oscillation was also realized in an atomic Raman system where two strong driving fields are present [14]. Recently, Rabi oscillation between photons of Raman write field and the

frequency-offset Stokes field was demonstrated [16] in Raman process where the driving field is a strong atomic spin wave. Here, the roles were reversed for atom and light as compared to the traditional Rabi oscillation effect. It was recently predicted [17] that Rabi-like coherent-superposition oscillation between light and atom can also occur in an atomic Raman process. When the driving field is a π-pulse, it is possible to make a complete conversion from light to atom for quantum storage or from atom to light for readout.

However, when the driving field is a $\pi/2$-pulse, we can achieve a coherent wave splitting of the input field into an optical wave and an atomic wave. The reverse process is just a coherent mixing of an optical wave and an atomic spin wave. Thus, it is possible to form a new type of interferometer made of atom and light. In contrast to the traditional interferometers, which are constructed with linear beam splitters for coherent splitting into a mixing of the same type of wave and are only sensitive to the phase shift of one type of wave, this new hybrid atom-light interferometer involves waves of different type and should depend on the phases of both optical and atomic waves. This is somewhat similar to an SU(1,1) type atom-light interferometer recently realized in our group [15]

In this paper, we report on the first observation of Rabi-like oscillation between light and atom in a Raman process involving Rb-atoms and a demonstration of an atom-light interferometer by employing this Rabi-like oscillation effect as atom and light wave splitter and mixer. This is a Ramsey-type interferometer in the sense that a strong driving laser in $\pi/2$-pulse area creates a superposition between atom and light and after a time delay with the evolution of both atom and light, another $\pi/2$-pulse laser is applied to mix atom and light for interference. In additional to the usual dependence on the optical phase, we find that the interference fringes also depend on the atomic phase, which is sensitive to a variety of physical quantities. Thus, this type of interferometer can be applied in precision measurement, sensitive measurement of atomic states, and quantum control of light and atoms.

The process we use to mix atomic and optical waves is the collective Raman process in an ensemble of N_a three-level atoms. The process is depicted in Fig.1a with the atomic levels and optical frequencies shown in Fig.1b. In the process, a pair of lower level meta-stable states $|g\rangle, |m\rangle$ is coupled to the Raman write field (W, or $\hat{a}_W$) and the Stokes field (S, or $\hat{a}_S$) via an upper excited level e. After adiabatically eliminating the upper excited level e, this process is a three-wave mixing process involving the write field, the Stokes field and a

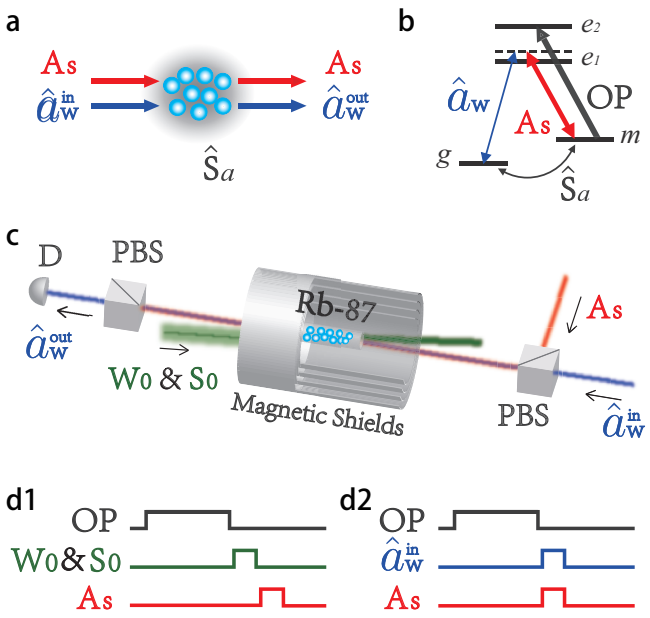

FIG. 1: **Experimental set-up of Rabi-like coherent oscillation. a.** Raman process for three-wave coupling of two optical fields (write $\hat{a}_W$ and Stokes A_S) and an atomic spin wave($\hat{S}_a$). **b.** Atomic energy levels for coupling optical fields. $|g\rangle$ and $|m\rangle$: two ground states $\left|5^2S_{1/2}, F=1,2\right\rangle$; $|e_1\rangle$ and $|e_2\rangle$: two excited states $\left|5^2P_{1/2}, F=2\right\rangle$ and $\left|5^2P_{3/2}\right\rangle$. OP: optical pumping field resonant on the $|m\rangle \rightarrow |e_2\rangle$ transition. **c.** Experimental arrangement for observing Rabi oscillation between atom and light driven by a strong Stokes field with the atoms having an initial spin wave. The initial spin wave is prepared by W_0&S_0 (see Method for detail). PBS: polarized beam splitter. **d1** and **d2** Timing sequences for the experiment with an initial spin wave $\hat{S}_a^{in}$ (d1) and a write field $\hat{a}_W^{in}$ (d2) as the only input field.

collective atomic pseudo-spin field $\hat{S}_a \equiv (1/\sqrt{N_a})\sum_k |g\rangle_k\langle m|$ and the coupling Hamiltonian is given by [18, 19]:

$$\hat{H}_R = i\hbar\eta\left(\hat{a}_W\hat{a}_S^\dagger\hat{S}_a^\dagger - \hat{a}_W^\dagger\hat{a}_S\hat{S}_a\right), \tag{1}$$

where $\eta = g_{eg}g_{em}/\Delta$ with g_{eg}, g_{em} as the coupling coefficients between the excited state and the lower level states. Δ is the detuning from the excited state for both the Stokes and Raman pump fields, which satisfy the two-photon resonance condition: $\omega_W - \omega_S = \omega_{mg}$. When the Stokes field $\hat{a}_S$ is very strong coherent field, replacing it with a c-number A_S in Eq.(1) and defining a Rabi-like frequency $\Omega = 2\eta A_S^*$, we have the Hamiltonian

$$\hat{H}_{BS}^{AL} = \frac{1}{2}i\hbar\left(\Omega^*\hat{a}_W\hat{S}_a^\dagger - \Omega\hat{a}_W^\dagger\hat{S}_a\right). \tag{2}$$

This Hamiltonian leads to the time evolution of the fields given by

$$\begin{aligned} \hat{a}_W^{out} &= \hat{a}_W^{in} \cos(\theta/2) + \hat{S}_a^{in} \sin(\theta/2), \\ \hat{S}_a^{out} &= \hat{S}_a^{in} \cos(\theta/2) - \hat{a}_W^{in} \sin(\theta/2), \end{aligned} \tag{3}$$

where θ is equal to $|\Omega|t$, with t the evolution time.

It is interesting to see that if there is only one input field, say the write field ($I_W^{(0)} \neq 0$), intensities of the output fields are $I_W = I_W^{(0)} \cos^2(\theta/2), I_{S_a} = I_W^{(0)} \sin^2(\theta/2)$, respectively, which oscillate in time with a frequency proportional to A_S, the amplitude of the strong Stokes field. This resembles the Rabi oscillation in a two level system driven by a strong field [12]. Here, the oscillation is between the write field and the atomic spin wave instead of the atomic levels while the strong Stokes field (A_S) is the driving field. Similar oscillation occurs if only the atomic spin wave is initially non-zero ($I_{S_a}^{(0)} \neq 0$): $I_W = I_{S_a}^{(0)} \sin^2(\theta/2), I_{S_a} = I_{S_a}^{(0)} \cos^2(\theta/2)$. On the other hand, if both fields are initially non-zero, the outputs are coherent mixture of the two fields with mixing coefficients as $\sin(\theta/2)$ and $\cos(\theta/2)$.

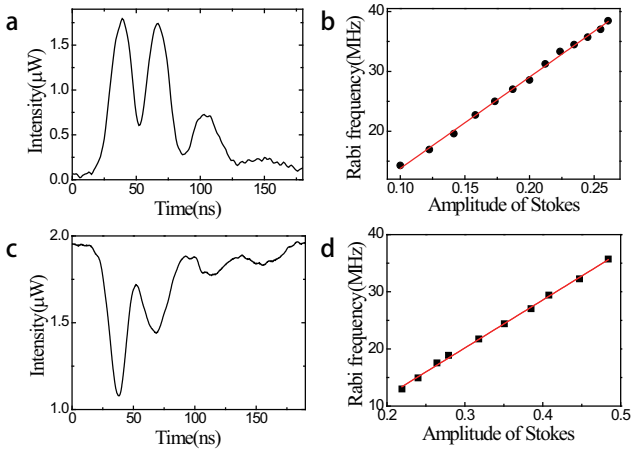

FIG. 2: **Results of Rabi-like oscillation between atom and light. a**. The output write field observed in time when the atomic spin wave has an initial value but no write field injection and **b.** the corresponding oscillation frequency as a function of the amplitude of the driving Stokes field. **c.** The observed output write field when the write field has an input but the atoms are all in the ground state and **d.** the corresponding Rabi oscillation frequency as a function of the amplitude of the driving Stokes field.

For the experimental observation of the Rabi oscillation between light and atom, we can approach by either preparing the atoms with an initial atomic spin wave or simply injecting a

write field. The experimental sketch is shown in Fig.1(c) with timing sequence in Fig.1(d1). In the first approach, atoms are initially prepared with a non-zero spin wave by two pulses of S_0 and W_0 (see Method for detail). After a short delay, a strong Stokes driving pulse (S) of 0.2 μs length is sent in opposite direction into the cell to drive the Rabi oscillation. To observe it, W-field ($\hat{a}_W^{out}$) is measured by a photo-detector and recorded in an oscilloscope. Fig.2(a) shows a typical run, clearly demonstrating the oscillation effect. The amplitude decay is due to the decoherence of the atomic spin wave. Fig.2(b) shows the oscillation frequency as a function of the amplitude A_S of the strong driving Stokes field. The linear dependence confirms it as a Rabi frequency, as given in Eq.(3). For the case of initial injection at the W-field ($\hat{a}_W^{in}$ shown in Fig.1), we need to lock its frequency to the strong Stokes driving field to within several hundred Hertz to satisfy the requirement of the two-photon resonance condition: $\omega_W - \omega_S = \omega_{gm}$. Time sequence is shown in Fig.1(d2). Fig.2(c) shows a typical run for this case. The oscillation frequency is confirmed in Fig.2(d) as Rabi frequency given in Eq.(3). Notice that the curves in Fig.2(a) and (c) are complementary to each other, reflecting the sine and cosine functions in Eq.(3).

From Eq.(3), we find when we adjust the pulse width or amplitude of the Stokes field so that $\theta = \pi$, the oscillation stops at the maximum conversion between atom and light. Notice that the input-output relation in Eq.(3) is exactly the relation for a lossless beam splitter [21, 22]: the write field here is equivalent to one of the input fields of the beam splitter and the atomic spin wave is the other field. Thus the outputs are coherent mixtures of the optical field and the atomic spin wave. When the pulse width satisfies $\theta = \pi/2$, only half will be converted and this leads to a coherent atom-light wave splitting.

Next, we use this atom-light wave splitter to form an atom-light interferometer. As shown in Fig.3, after the first splitting of the incoming wave (the initially prepared atomic spin wave here in our experiment), we mix the split atom and light waves with another but similar conversion process. This is done by redirecting the generated W-field (W_1) back to the atomic cell which contains the unconverted atomic spin wave and mixing them with another Stokes $\pi/2$-pulse. To separate the splitting and the mixing processes, a delay between the two Stokes $\pi/2$ pulses is introduced with a 100-meter-long single mode fiber (SMF_0). Similar delay with another SMF_1 is introduced in the returned W-field.

To make a comparison with a conventional interferometer with beam splitters, the first pulse will act as the Raman read field in the first Raman read process to split the initially

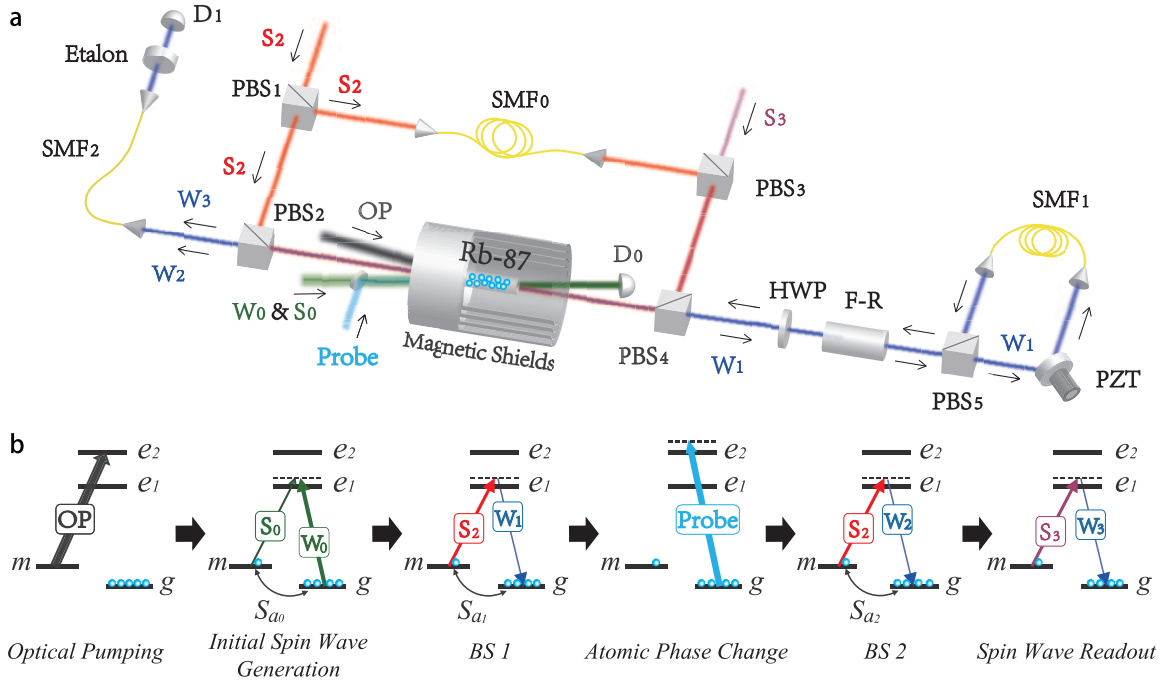

FIG. 3: **Atom-light hybird interferometer. a.** Experimental set-up and **b.** atomic energy levels with frequencies of optical fields for the formation of an atom-light hybrid interferometer. HWP: half wave plate; F-R: Faraday rotator. PZT: Piezoe-lectric Transducer; SMF: single-mode fiber. W_1, W_2, W_3: write fields; S_2, S_3: strong Stokes fields. BS1: the first splitting process to split the initial spin wave S_{a0} to coherent superposition of write field W_1 and spin wave S_{a1}. BS2: the second beam splitting process to mix W_1 and S_{a1} and output W_2 and S_{a2}.

prepared atomic spin wave S_{a0} into half write field (W_1) and half spin wave (S_{a1}). This process can be regarded as the first beam splitter in the conventional interferometer. The lengths of the two SMFs are made equal to ensure that the delayed Stokes pulse (S_2) and the write field W_1, generated in the first Raman process and fed-back to the cell, will enter the vapor cell that contains the spin wave S_{a1} at the same time to carry out the second Raman process for mixing S_{a1} and W_1, i.e., the second beam splitter process. In between the first splitting and the second mixing processes, we introduce a phase modulation unit (PZT) in W_1's path to change its phase. The final light signal in the write field (W_2) after the second BS is collected with another single mode fiber (SMF_2) and detected after an

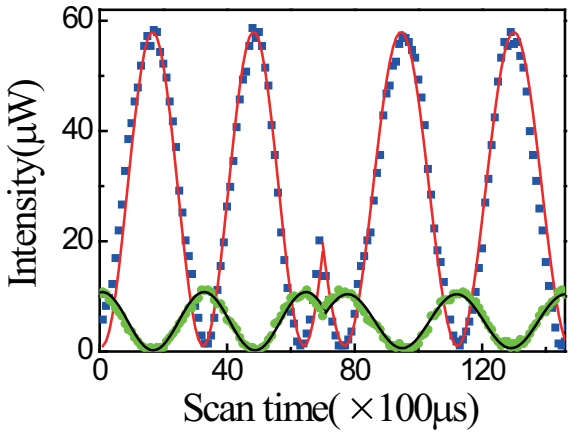

FIG. 4: **Interference fringes of atom-light hybrid interferometer.** Observed interference fringes at the output write field (blue squares) and for the final atomic spin wave (green dots) as the optical phase is scanned via a ramp voltage on the PZT.

etalon, which is used to filter out the leaked strong Stokes photons. The atomic signal after the second BS can be converted into the light field (W_3) by injecting another strong read pulse (S_3) right after the second Stokes pulse (S_2). The conversion efficiency is about 20%. This signal is also collected by SMF_2 and detected after the etalon. So we will observe two temporally separated pulses by the detector: first one from W_2 and second one from W_3. The heights of the two pulses correspond to the intensities of the final write field (W_2) and the final atomic spin wave S_{a2}, respectively. Fig.4 shows the interference fringes detected in both the output W-field and the final atomic spin wave. The solid lines are the best fits to the cosine function with visibilities of 96.6% and 94.8%, respectively.

Since the atomic spin wave is involved in this interference scheme, the interference fringes should depend on the phase of the atomic spin wave as well, which can be changed by some external field, such as magnetic field and electric field. However, dependence on the magnetic field relies on the magnetic sub-levels and can be very complicated. Here, we resort to an AC Stark effect [23] for the atomic phase change. It is well-known that when atoms are subject to the illumination of an electromagnetic field, their energy level will be shifted. For the atomic Raman process discussed previously, the AC Stark shift is given by the amount of [19]

$$\Delta\Omega_{AC} = g_{eg}g_{em}|E|^2/\Delta, \tag{4}$$

where E is the amplitude of the field and Δ is the detuning. This will lead to a phase

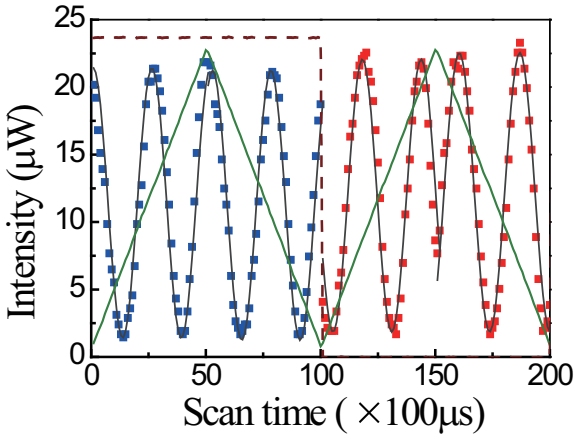

FIG. 5: **AC Stark effect on interference output.** Interference fringes at the output write field with (blue) and without (red) the atomic phase shift induced by the AC Stark effect. Green lines are the ramp voltage on the PZT for phase scan and the dotted lines are for probe light intensity (scales are not drawn for both lines)

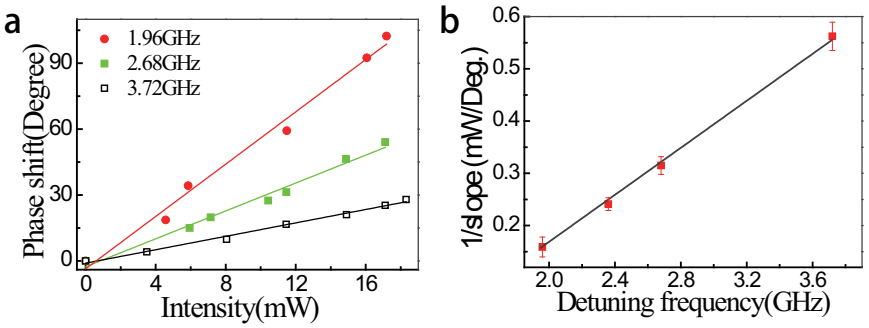

FIG. 6: **Atomic phase shift. a.** The induced phase shift as a function of the intensity of the inducing light field (probe). **b.** The inverse of the slopes of the linear fits from (a) as a function of detuning frequency of probe field.

shift of $\Delta\varphi = \Delta\Omega_{AC}\Delta T$ for an interaction time of ΔT. Thus, the atomic phase is directly proportional to the intensity $I \propto |E|^2$ of the applied field and the optical delay ΔT. In the experiment, the external field (called as probe) comes from another laser at 780 nm tuned to D2 line with 2 to 3 GHz detuning. We turn on the laser after the first Raman splitting process for $\Delta T = 80$ ns and turned it off right before the second Raman mixing process. In this way, the phase-shifting field will not affect the Raman processes for splitting and mixing the atomic and optical waves. Fig.5 shows two interference fringes with and without the 780nm-laser turned on. The laser power is about 45 mW. We can extract a phase shift

of 2.5 radian from the two fringes. In Fig.6(a), we plot the phase shift as a function of the intensity of the 780nm-laser at various detuning. Then the inverse of the slopes of the linear fits from Fig.6(a) are plot against the detuning. The linear dependence shown in both Fig.6(a) and (b) is in agreement with Eq.(4). From Fig.6, we find $\Delta\varphi = \kappa P \Delta T/\Delta$ with $\kappa = 0.06 Degree \cdot GHz/ns \cdot mW$ for $\Delta T = 80$ ns.

In summary, we demonstrate coherent conversion between atom and light in the form of a Rabi-like oscillation. This coherent conversion process can be used as a wave splitter into coherent superposition of atomic spin wave and optical wave and as a wave mixer of the coherent atomic spin wave and optical wave. We construct an atom-light hybrid interferometer in which the interference fringes depend on both the optical phase and atomic phase. The intensity-dependent atomic phase shift can be used for a quantum non-demolition measurement (QND) [24–26] of the photon number of the phase-inducing field (the 780nm-laser beam in our experiment). This is similar to the QND measurement in optical Kerr effect [27–29]. Furthermore, atomic phase can be changed by other means such as magnetic and electric field. So, this atom-light interferometer will have wide applications in precision measurement, quantum metrology, and quantum control of atom and light.

Method

In the experiment, the atomic medium is Rubidium-87 atoms which is contained in a 50mm long paraffin coated glass cell. The cell is placed inside a four-layer magnetic shielding to reduce stray magnetic fields and is heated up to 75° using a bi-filar resistive heater. The energy levels of the Rb atom are shown in Fig.3b, where states $|g\rangle$ and $|m\rangle$ are the two ground states ($5^2S_{1/2}F = 1, 2$) from hyperfine splitting and $|e_1\rangle, |e_2\rangle$ are two excited states ($5^2P_{1/2}, 5^2P_{3/2}$). An optical pumping field (OP), tuned to $|m\rangle \rightarrow |e_2\rangle$ transition at 780 nm, is used to prepare the atoms in $|g\rangle$ state. To get the initial atomic spin wave S_{a0}, we apply the Raman write field (W_0) and Stokes seed (a_{S0}) simultaneously to perform a stimulated Raman scattering. The write laser is blue-detuned about 1.5 GHz from $|g\rangle \rightarrow |e_1\rangle$ transition. The Stokes seed we used comes from the same laser as the W_0 beam but its frequency is red-shifted 6.8 GHz from W_0 beam in another vapor cell using feedback Raman scattering [20].

*lqchen@phy.ecnu.edu.cn

†zou@iupui.edu

‡wpzhang@phy.ecnu.edu.cn

---

[1] Fleischhauer, M. & Lukin, M. D. Dark-state polaritons in electromagnetically induced transparency. *Phys. Rev. Lett.* **84**, 5094 (2000).

[2] Liu, C., Dutton, Z., Behroozi, C. H. & Hau, L. V. Observation of coherent optical information storage in an atomic medium using halted light pulses. *Nature* **409**, 490 (2001).

[3] Phillips, D. F., Fleischhauer, A., Mair, A., Walsworth, R. L. & Lukin, M. D. Storage of light in atomic vapor. *Phys. Rev. Lett.* **86**, 783 (2001).

[4] Mair, A., Hager, J., Phillips, D. F., Walsworth, R. L. & Lukin, M. D. Phase coherence and control of stored photonic information. *Phys. Rev. A* **65**, 031802(R) (2002).

[5] Honda, K. *et. al.* Storage and retrieval of a squeezed vacuum. *Phys. Rev. Lett.* **100**, 093601 (2008).

[6] Appel, J., Figueroa, E., Korystov, D., Lobino, M. & Lvovsky, A. I. Quantum memory for squeezed light. *Phys. Rev. Lett.* **100**, 093602 (2008).

[7] Nunn, J. *et. al.* Mapping broadband single-photon wavepackets into an atomic memory. *Phys. Rev. A* **75**, 011401(R) (2007).

[8] Reim, K. F. *et. al.* Towards high-speed optical quantum memories. *Nature Photonics* **4**, 218 (2010).

[9] Reim, K. F. *et. al.* Single-photon-level quantum memory at room temperature. *Phys. Rev. Lett.* **107**, 053603 (2011).

[10] Reim, K. F. *et. al.* Multipulse addressing of a raman quantum memory: configurable beam splitting and efficient readout. *Phys. Rev. Lett.* **108**, 263602 (2012).

[11] Campbell, G., Hosseini, M., Sparkes, B. M., Lam, P. K. & Buchler, B. C. Time- and frequency-domain polariton interference. *New J. Phys.* **14**, 033022 (2012).

[12] Allen, L. & Eberly, J. H. *Optical Resonance and Two-level Atoms* (John Wiley and Sons, New York, 1975).

[13] Ramsey, N. F. A molecular beam resonance method with separated oscillating fields. *Phys. Rev.* **78**, 695 (1950).

[14] Loy, M. M. T. Observation of population inversion by optical adiabatic rapid passage. *Phys. Rev. Lett.* **32**, 814 (1974).

[15] Chen, B. *et. al.* Atom-light hybrid interferometer. *Phys. Rev. Lett.* **115**,043602 (2015).

[16] Chen, L. Q. *et. al.* Observation of the Rabi oscillation of light driven by an atomic spin wave. *Phys. Rev. Lett.* **105**, 133603 (2010).

[17] Ou, Z. Y. Efficient conversion between photons and between photon and atom by stimulated emission. *Phys. Rev. A* **78**, 023819 (2008).

[18] Duan, L. M., Lukin, M. D., Cirac, J. I. & Zoller, P. Long-distance quantum communication with atomic ensembles and linear optics. *Nature* **411**, 413 (2001).

[19] Hammerer, K., Sorensen, A. S. & Polzik, E. S. Quantum interface between light and atomic ensembles. *Rev. Mod. Phys.* **82**, 1041 (2010).

[20] Chen, B. *et. al.* Efficient Raman frequency conversion by coherent feedback at low light intensity. *Opt. Exp.* **21**, 010490 (2013).

[21] Ou, Z. Y., Hong, C. K. & Mandel, L. Relation between input and output states for a beam splitter. *Opt. Commun.* **63**, 118 (1987).

[22] Campos, R. A., Saleh, B. E. A. & Teich, M. C. Quantum-mechanical lossless beam splitter: SU(2) symmetry and photon statistics. *Phys. Rev. A* **40**, 1371 (1989).

[23] Autler, S. H. & Townes, C. H. Stark effect in rapidly varying fields. *Phys. Rev.* **100**, 703 (1955).

[24] Braginsky, V. B., Vorontsov, Y. I. & Thorne, K. S. Quantum nondemolition measurements. *Science* **209**, 547 (1980).

[25] Porta, A. L., Slusher, R. E. & Yurke, B. Back-action evading measurements of an optical field using parametric down conversion. *Phys. Rev. Lett.* **62**, 28 (1989).

[26] Pereira, S. F., Ou, Z. Y. & Kimble, H. J. Backaction evading measurements for quantum nondemolition detection and quantum optical tapping. *Phys. Rev. Lett.* **72**, 214 (1994).

[27] Levenson, M. D. *et. al.* Quantum nondemolition detection of optical quadrature amplitudes. *Phys. Rev. Lett.* **57**, 2473 (1986).

[28] Friberg, S. R. *et. al.* Quantum-nondemolition measurement of the photon number of an optical soliton. *Phys. Rev. Lett.* **69**, 3165 (1992).

[29] Poizat, J. Ph. & Grangier, P. Experimental realization of a quantum optical tap. *Phys. Rev. Lett.* **70**, 271 (1993).

Acknowledgements

This work was supported by the National Basic Research Program of China (973 Pro-

gram) under Grant No. 2011CB921604, the National Natural Science Foundation of China (Grant No. 11274118, 91536114, 11129402 and 11234003) and Supported by Innovation Program of Shanghai Municipal Education Commission (Grant No. 13ZZ036).

Author contributions

CQ, SC, BC and JG performed the experiment under the supervision of LQC and ZYO. CQ, SC, LQC analyzed the data. LQC, ZYO and WPZ wrote the paper. WPZ provides the overall supervision on this project.